Quantitative Molecular Analysis with Molecular Bands Emission using Laser-Induced Breakdown Spectroscopy and Chemometrics

Doucet, François; Faustino, Patrick J.; Sabsabi, Mohamad; Lyon, Robbe C.

Publisher's version / Version de l'éditeur:
http://dx.doi.org/10.1039/b714219f
Journal of Analytical Atomic Spectrometry, 23, 5, pp. 694-701, 2008

Quantitative molecular analysis with molecular bands emission using laser-induced breakdown spectroscopy and chemometrics

François R. Doucet,*[a] Patrick J. Faustino,[b] Mohamad Sabsabi[a] and Robbe C. Lyon[b]

Received 14th September 2007, Accepted 19th February 2008
First published as an Advance Article on the web 7th March 2008
DOI: 10.1039/b714219f

The present work describes the first quantitative molecular prediction using laser-induced molecular bands along with chemometrics. In addition, this spectroscopic procedure has demonstrated the first complete quantitative analysis utilizing traditionally insensitive elements for pharmaceutical formulations. Atomic LIBS requires certain sensitive elements, such as Cl, F, Br, S and P, in order to quantitate a specific organic compound in a complex matrix. Molecular LIBS has been demonstrated to be the first successful approach using atomic spectroscopy to evaluate a complex organic matrix. This procedure is also the first quantitative analysis using laser-induced molecular bands and chemometrics. We have successfully applied chemometrics to predict the formulation excipients and active pharmaceutical ingredient (API) in a complex pharmaceutical formulation. Using such an approach, we demonstrate that the accuracy for the API and a formulation lubricant, magnesium stearate, have less than 4% relative bias. The other formulation excipients such as Avicel® and lactose have been accurately predicted to have less than a 15% relative bias. Molecular LIBS and chemometrics have provided a novel approach for the quantitative analysis of several molecules that was not technically possible with the traditional atomic LIBS procedure, that required sensitive elements to be present in both API and formulation excipients.

Introduction

The use of laser-induced breakdown spectroscopy (LIBS) for qualitative analysis of organic material is currently a subject of great interest in the LIBS community. However, the quantitative analysis of organic compounds has not been reported yet using LIBS spectral data and chemometrics. The combination of chemometrics and LIBS has shown promising results for rapid at-line multielemental quantitative analysis of aluminium alloys using abundant certified reference materials.[1] There have been a number of wide ranging qualitative applications of LIBS for organic compounds which include polymers,[2,3] inks,[4] hydrocarbons[5] and coral beads.[6] The topic that receives the most attention is the use of LIBS for standoff analysis of explosive residues and biological material for homeland security applications.[7–22] Many approaches have been proposed for qualitative analysis of explosive residues.[7–12,19,20,22] In particular, the use of atomic ratio of neutral lines of nitrogen, oxygen and carbon[10–14,19,20,22] have been used for the differentiation of explosives residues. However, these approaches have been hindered by the atmospheric gases which are composed mainly of nitrogen, and oxygen elements commonly found in non-metallic organic materials. This has been a challenging technical problem for standoff detection of organic material in air. To overcome these issues, some researchers have proposed to include emission bands of CN and C_2 to the atomic ratio criterion for discrimination of explosive residue spectra under atmospheric conditions.[10–14] These approaches, along with the use of clustering techniques[16–20,22] and spectral database searches,[10–12] have been evaluated and suggest promise. Recently, Schade and Bohling have proposed following the temporal emission decay of molecular bands of CN along with an artificial neural network approach to differentiate different explosive residues.[7,8] The multiplicity of research approaches and multivariate analysis techniques show the fundamental interest in utilizing LIBS as an analytical technique for the standoff detection of organic compounds.

In the pharmaceutical arena, the story begins in 1998 with the patent of Sabsabi and Bussière that describes a spectroscopic method and apparatus for pharmaceutical analysis.[23] Soon after, a wide range of pharmaceutical applications for LIBS began to emerge.[24–32] These applications include the monitoring of the active pharmaceutical ingredients (API) and a formulation lubricant such magnesium stearate[29] as well as the possibility of generating the first results capable of globally mapping pharmaceutical solid dosage forms.[26] As is typical in NIR and Raman reflectance spectroscopy, pure components are analysed before their preparation in a solid dosage form. Although, for these baseline spectral techniques, it has been shown that physical properties, such as particle size, will result in spectral diffusion that limits the applicability of these baseline spectra to facilitate the differentiation of physical changes from chemical or compositional changes that may result from the combination of these components into a formulation.[33–35] Additionally, matrix effects and excipient interactions may limit the use of these reflectance

[a]*National Research Council Canada, Industrial Materials Institute, 75 de Mortagne Blvd., Boucherville (QC), Canada J4B 6Y4. E-mail: francois.doucet@cnrc-nrc.gc.ca*
[b]*US Food and Drug Administration, Center for Drug Evaluation and Research, Division of Product Quality Research, Silver Spring, MD, 20993, USA*

baseline spectra and affect overall spectral information.[33–35] With molecular LIBS spectroscopic analysis we have shown good selectivity for those pharmaceutical formulation constituents without the need of baseline spectra.[30] Well established reflective spectroscopic techniques such as NIR and Raman are also hindered by the penetration depth at the solid dosage form surface.[36–38] Whereas LIBS has the distinct ability to selectively obtain information at the tablet surface and throughout the entire tablet without spectral diffusion that is usual with NIR and Raman transmission techniques.

Another important application of LIBS for pharmaceutical materials is the analysis of coating thickness and uniformity on the tablet[26] for rapid at-line analysis for enhanced process control. LIBS has also been applied to the on-line monitoring of liquid pharmaceutical formulations,[28] which have demonstrated the on-line/in-line process monitoring capability of LIBS. It is only as recently as 2006 that LIBS applications for pharmaceutical materials were first reviewed in a book chapter.[25] The technique has also been compared to traditional analytical techniques, such as scanning electron microscope coupled with energy dispersive X-ray emission (SEM-EDX)[31] and with near-infrared (NIR) spectroscopy, for determination of magnesium stearate, a critical formulation ingredient necessary for ensuring product performance.[32] The efforts of these early LIBS researchers have highlighted the presence of the "matrix effect". To overcome the matrix effect resulting primarily from physical property variations induced by the manufacturing changes on solid dosage forms, efforts have been made to understand the influence of many parameters on the LIBS signals.[24,27,39] These atomic LIBS studies agree that the use of matrix-matched calibration standards are necessary to overcome the matrix effect to produce accurate quantitative results.[24,27,39,40] Since atomic LIBS signals can be affected by many physical parameters in the manufacturing process, traditionally known as matrix-effects, two research studies[24,27] have demonstrated that the LIBS technology is a valuable tool for process analytical technologies. The matrix effect is sensitive enough to be utilized for an in-process monitoring approach for pharmaceutical manufacturing.[39,40]

The basic hypothesis of the molecular LIBS approach developed here is that the emission from small molecular fragments coming from the laser-induced plasma are characteristic of the parent molecules fragmented in the creation of the latter. It is well known that the fragmentation of a molecule is a function of the chemical bonding and the functional groups present in the molecule. The fundamental molecular structure, the nature of the bonds, the conformation, and the isomers contribute to the specific nature of the molecular emission. We propose to use the emission signal from the small molecular fragments coupled with chemometrics to evaluate the primary chemical structures in pharmaceutical formulations. Using favorable experimental conditions, the fragmentation will produce selective daughter molecular fragments from the primary or parent molecule. Molecular bands emission will be used, for the first time to the best of our knowledge, for the determination of the chemical moieties and the evaluation of the chemical structure of both the API and excipients in a complex pharmaceutical formulation. Molecular LIBS is an information rich multiplex spectral technique which contains both atomic and molecular emission spectra that, following analysis by multivariate approaches (*i.e.* chemometrics), will extract this unique combination (molecular, atomic, ionic) of spectral information from molecular LIBS. Additionally, molecular LIBS is able to avoid many of the classical spectroscopic limitations such as light scattering, diffusion, absorption, penetration depth, sample preparation, material type, *etc.* These inherent advantages provide a broader range of problem solving capability (*e.g.* accurate depth profiling, 3D chemical mapping, direct solid, liquid and gas analysis) and can be used for in-process control (raw materials), process control (blending, mixing, tableting), process understanding, process analytical technology (PAT), quality by design (QbD), risk management and quality assurance. Although this work focuses primarily on pharmaceutical applications, the potential for molecular LIBS transcends pharmaceuticals and extends analytical science, opening the door to many useful applications.

This study investigated the laser-induced molecular bands emission coupled with chemometrics for the qualitative and quantitative analysis of molecular compounds found in a model pharmaceutical formulation. Our goal is to establish laser-induced plasma conditions that enhance selective emission of molecular fragments from the sample. By doing so, we can analyze the photons emitted by small diatomic fragments with a conventional optical spectrometer that will be mathematically processed with chemometrics to study the parent compounds, such as API and excipients, simultaneously. To the best of our knowledge, this spectroscopic approach is the first documented effort to conduct qualitative and quantitative analysis of both API and excipients simultaneously using laser-induced breakdown spectroscopy or with any other atomic emission spectroscopy based techniques.

Experimental

Apparatus and materials

A Nd:YAG laser operating at 1064 nm (Surelite II-10, Continuum, Santa Clara, CA, USA) producing pulses of 6 ns duration (full width at half maximum) was used. The pulse energy at the laser exit was 100 mJ. The laser beam was focused on the tablet surface using a plano-convex lens (515 mm focal length), producing crater diameters of approximately 500 μm. The horizontal beam was incident on the vertical tablet surface at 90° as represented in Scheme 1.

The tablet was held in a custom-made sample holder which could accommodate 12 mm tablet. The sample holder was mounted on a motorized X–Y stage, allowing programmable analysis at several sites on a given tablet. The experiments were performed in argon at atmospheric pressure using a 1 L min^{-1} argon flow on the target. The light given off by the laser-induced plasma was collected head-on by a mirror and then directed to a 0.66-m Czerny-Turner spectrometer (McPherson, Acton, MA, USA). Using a lens, the plasma was imaged with 1 : 2 magnification on the entrance slit of the spectrometer, which is equipped with a 150 grooves per mm grating blaze at 500 nm. The dispersed light was detected at the exit slit of the spectrograph with an intensified photo-diode array (IPDA) (Princeton Instruments, Trenton, NJ, USA)

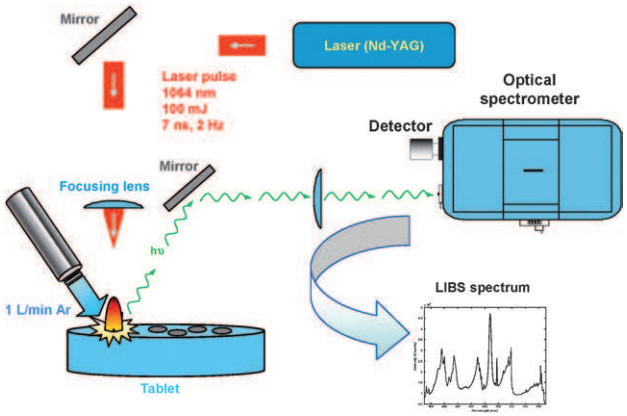

Scheme 1 Simplified representation of the experimental set-up.

detector. The emission signal was time-resolved using a pulse generator (Princeton Instruments, model PG-200) (itself synchronized with the laser pulse) by sending a gating signal to the intensifier with a delay of 4 μs and a pulse width of 750 ns, these conditions were found to be optimal regarding the signal to noise ratio and repeatability of the analytical signals.

The pulse repetition rate was 2 Hz, allowing 99 measurements on a given tablet to provide a representative average compositional analysis in less than 50 seconds for the 3 × 3 raster (*i.e.* 9 sampling sites × 11 shots per site = 99 laser shots per sample). Each laser shot produced 726 pixel intensities that were averaged ($n = 90$) for each sample without the first shot at each site ($n = 9$), to avoid any potential surface contamination. Therefore, a sample spectra composed of 726 mean pixel intensities resulting from 90 laser shots per sample was stored for each analyzed standard. The dependent variable matrix for the calibration set was composed of 90 spectra (*i.e.* 15 standards × 6 replicates, formulation A to O, Table 1) and 18 spectra (*i.e.* 3 standards × 6 replicates, formulation P to R, Table 1) for the validation set. The corresponding independent variable matrix was built from the data presented in column 4 to 7 from Table 1 (*e.g.* for the calibration set: 90 standards × 4 components). Thereafter, this matrix of data was introduce into PLS or PCR models and pre-processed if necessary as specified in the text.

The experimental set-up and spectral data were controlled using a custom application developed in LabVIEW 6 (National Instruments, Austin, TX, USA). Spectral data post-treatment with chemometrics was performed using a custom algorithm under Matlab 7.5 environment (The MathWorks Inc., Natick, MA, USA). The Matlab built-in singular value decomposition (SVD) function was used in order to extract the principal components used for the construction of principal component regression (PCR). For the construction of partial least square (PLS) regression a PLS2 model was used.[41]

Calibration standards

For each standard, 6 replicate tablets were prepared. The powder mixing was done by mortar and pestle mixing for 5 minutes using the formulation quantities presented in Table 1. The solid dosage form tablets were prepared by compressing 320 mg of powder with 2000 psi (Enerpac, P112, Whaley Bridge, High Peak, UK) for 15 s. The furosemide API used in the model formulation was Lot 36 H0944 (Sigma-Aldrich, St-Louis, MO, USA). Avicel PH 101 (Lot 6108C), (FMC BioPolymer, Philadelphia, PA, USA) was used with lactose 200 M monohydrate (Lot M00448), (Mallinckrodt, St. Louis, MO, USA) as excipients. Magnesium stearate (Lot M00295, Mallinckrodt) was used in the formulation as lubricant.

Safety considerations

It is important to note that there are some safety considerations and the reader is invited to consult ref. 42–44 for more information.

Table 1 Composition of the model formulation

Standard name	Lactose in matrix (%)	Furosemide (% of nominal)	Furosemide/mg	Lactose/mg	Avicel®/mg	Mg Stearate/mg
A	0	80	64	0	255.2	0.8
B	0	100	80	0	239.2	0.8
C	0	120	96	0	223.2	0.8
D	50	80	64	127.6	127.6	0.8
E	50	100	80	119.6	119.6	0.8
F	50	120	96	111.6	111.6	0.8
G	100	80	64	255.2	0	0.8
H	100	100	80	239.2	0	0.8
I	100	120	96	223.2	0	0.8
J	0	80	64	0	253.2	2.8
K	50	100	80	118.6	118.6	2.8
L	100	120	96	221.2	0	2.8
M	0	80	64	0	249.6	6.4
N	50	100	80	116.8	116.8	6.4
O	100	120	96	217.6	0	6.4
P[a]	25	90	72	61.75	185.25	1
Q[a]	75	110	88	171	57	4
R[a]	40	85	68	100	150	2

[a] Standard used as validation standard.

Results and discussion

Selectivity of the laser-induced plasma

The chemical structures of the molecules studied with the model formulation are presented in Scheme 2. It should be quickly noted that the furosemide molecular structure is the only one that contains target sulfur, nitrogen and chlorine atoms when compared to the other molecular structures of the excipients present in the model formulation, such as magnesium stearate, Avicel® and lactose.

The traditional approach for the analysis of the active pharmaceutical ingredient (API) was to monitor the emission signal of a target element.[29] Therefore, the peak height or peak area of the signal resulting from sulfur or chlorine atomic lines, in the case of furosemide, can be plotted against the concentration to produce a calibration curve for quantification of furosemide. The advantage of such an univariate approach is that it uses simple mathematics for calibration and therefore a quantitation approach that is generally well understood by the analyst in the laboratory. However, this approach requires matrix-matched calibration standards to produce an accurate prediction.[24,27]

Following the set-up of a favorable argon atmosphere that will minimize the contribution of air to the laser-induced plasma and at the same time enhance the molecular band emission signal, we performed the molecular LIBS spectroscopic experiments on a series of model formulations composed of furosemide, Avicel®, lactose and magnesium stearate. Avicel® and lactose are pharmaceutical excipients (inactive pharmaceutical ingredients) that represent typically 80 percent of the total mass of a pharmaceutical solid dosage form. In analytical chemistry, these excipients are named the matrix since they are the major constituents of the sample other than the analytes. Characteristic spectra produced from a laser-induced plasma from a furosemide pharmaceutical formulation is presented in Fig. 1. It is important to note that these characteristic spectra are highly reproducible (RSD% for the spectra varies between 0.45 to 2.7% depending on the camera pixels for 6 standard replicates) with low resolution (resolving power $\lambda/\Delta\lambda \sim 700$ based on 3 pixels) that provides the required selectivity for building the chemometric models. The performance of this approach is comparable to traditional molecular spectroscopic procedures.

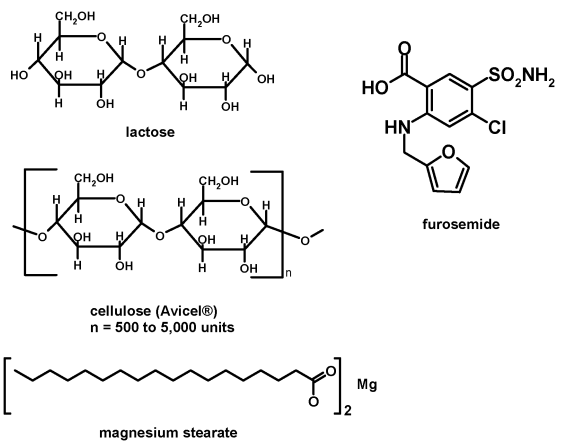

Scheme 2 Chemical structures of the different molecular compounds present in the model furosemide formulations.

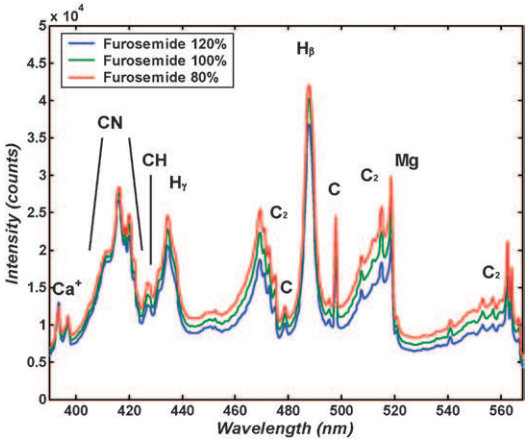

Fig. 1 Molecular LIBS spectra obtained for different active pharmaceutical ingredient concentrations in the furosemide formulation (lots G, H and I).

The spectra presented in Fig. 1 show the emission of many small diatomic fragments such as CN, CH and C_2 for a constant matrix composed of pure lactose as the excipient. Furthermore, it is also possible to observe the presence of atomic lines of carbon, hydrogen and magnesium and two ionic lines of calcium. The laser-induced spectra presented in Fig. 1 shows the LIBS response for 80, 100 and 120% of the label claim for furosemide while the other excipients remain constant with 100% lactose. It is possible to observe that the tree series of molecular bands of C_2 (roughly between 455–475 nm, 500–520 nm and 540–565 nm) vary with the increase of the API concentration. The emission of the C_2 bands is in agreement with previous univariate work which associates the C_2 emission with the presence of the unsaturation in the molecule.[30] On the other hand, the two ionic lines of calcium at 393 and 397 nm in Fig. 1 remain constant. The other molecular bands of CN and CH in addition with the atomic lines of H and C in Fig. 1 are less affected by the increase of the API concentration. These spectral behaviors indicate a correlation between variables for which chemometric models are presently uniquely capable of processing; which clearly demonstrate the information rich nature of molecular LIBS spectra.

The CN molecular bands emission is a result of the furosemide fragmentation and the recombination between C and N atom in the plasma. Since, the experiments were conducted under argon atmosphere, the CN emission from the recombination of these atomic species present in the plasma should not come from the recombination between C_2 in the plasma and N_2 from the air. St Onge *et al.* have demonstrated the kinetic evidence of this recombination reaction in air to produce CN.[30] Therefore, the CN emission signal is a result of the elemental and molecular nature of the plasma. Hence, the CN emission can be primarily attributed to the presence of furosemide molecules. Nitrogen is present in furosemide, but it is not present in lactose, cellulose, or magnesium stearate. Consequently, the CN emission can be primarily attributed to the presence of furosemide in the ablated sample. If we theoretically infer, as suggested by Acquaviva, that the CN emission origin was a result from some other nitrogen contamination from the air ($N_{2\ air\ or\ adsorb}$).[45] Then, following this reaction:[30]

$$C_{2\ plasma} + N_{2\ air\ or\ adsorb} \rightarrow 2\ CN_{plasma} \quad (1)$$

it can be reasonably inferred that this spectral contribution won't be correlated to the presence of furosemide. Therefore, the multiplex signal generated by the mixed matrix standards accurately describes the furosemide in the formulation. In addition, this CN contribution (eqn (1)) to the LIBS spectra will be relatively constant with a small random variation. It will not significantly impact the accurate quantitative analysis of the furosemide molecules. Therefore, multivariate regression models such PLS and PCR would not capture this part of the spectra, leaving it in the residual with the noise and the uncorrelated spectral variations.[41]

We present in Fig. 2 the mean emission spectra obtained for 6 replicate spectra of our model pharmaceutical formulations containing 3 different Avicel®/lactose ratios while maintaining the API (at 100% of the nominal content in furosemide) and lubricant concentration constant. It is possible to observe that the molecular bands present between 390 to 520 nm are sensitive to changes in the matrix composition. The two calcium ionic emission lines observed as the net intensity at 393 and 397 nm are inversely proportional to the Avicel® content. This indicates that lactose contains more calcium than the Avicel® which seems obvious since lactose is generally extracted from milk. Interestingly, the presence of Avicel® seems to contribute globally to the emission bands and atomic lines in this spectroscopic window. In fact, the presence of Avicel® impacts the entire spectrum presented in Fig. 2 in the same spectroscopic pattern as lactose. The latter observation can be quite obvious when considering the characteristics of the molecular structures of Avicel® and lactose presented in Scheme 2. The chemical building block of Avicel® (cellulose) is nearly identical to the structure of lactose, the differences consist of two fewer hydrogen, and that Avicel® is a polymer containing between 500 and 5000 units whereas lactose is a dimer. On the other hand, this does not explain the significant signal intensity difference observed for these two materials. A reasonable explanation for this phenomenon may be that since Avicel® is a polymer, the fragmentation might be less effective, producing more molecular fragments. In other words, the fragmentation for lactose leads to the greater production of atoms and ions and less molecular fragments than in the case of Avicel®.

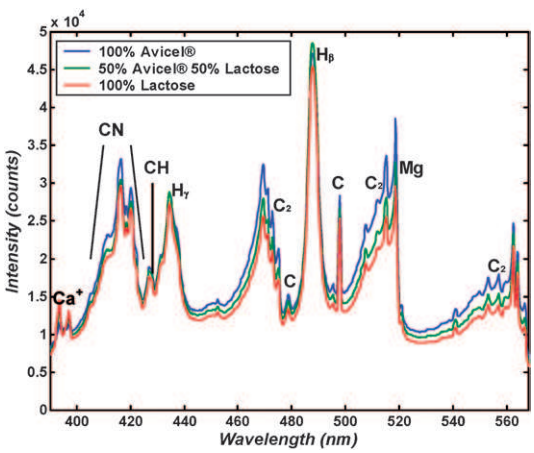

Fig. 2 Molecular LIBS spectra obtained for different major excipients composition in the furosemide (nominal 100%, lots B, E and H).

Construction of chemometrics model

The molecular LIBS spectroscopic data presented in Fig. 1 and Fig. 2 highlight the physico-chemical properties and the statistical requirements required for the building of a reliable chemometrics model as recommended by Gemperline.[41] The molecular LIBS emission spectra obtained for the calibration set and the validation set are presented in Fig. 3.

It is possible to observe each distinct individual mean spectrum ($n = 6$) in Fig. 3 which reveals the selectivity of the molecular LIBS emission spectra for the different standards using this spectral window. The individual spectra were used for constructing the chemometric calibration (formulation A to O) and validation (formulation P to R) sets. The evaluation of various data pre-treatments (*i.e.* raw data, mean-centering, range scaling and auto-scaling) for principal component regression (PCR) and partial least square (PLS) is presented in Table 2. This table reports the corresponding root mean square error of calibration (RMSEC), the root mean square error of prediction

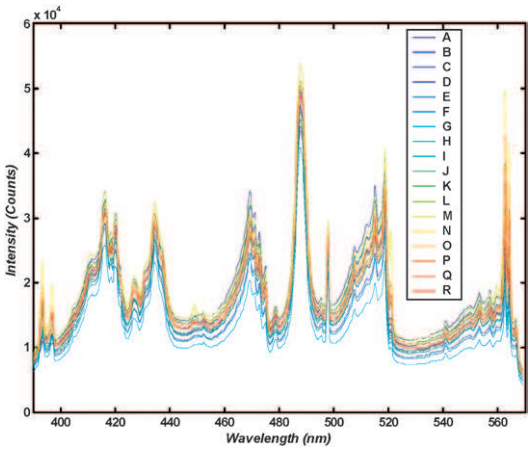

Fig. 3 Mean molecular LIBS spectra obtained for the calibration and validation standard sets average spectra ($n = 6$) for the model formulations presented in Table 1. The individual spectra were used for constructing the chemometric calibration and validation sets.

Table 2 Evaluation of PCR and PLS for different data pre-treatments

Data pre-treatment	nLV[a]	Furosemide RMSEC[b]/mg	Furosemide RMSEP[c]/mg	R^{2d}
PCR				
Raw data	10	6.36	6.64	0.956
Mean centering	9	7.32	5.98	0.935
Range scaling	8	6.56	6.71	0.954
Auto-scaling	7	5.99	6.88	0.959
PLS				
Raw data	5	11.0	5.94	0.952
Mean centering	5	5.93	9.99	0.929
Range scaling	5	7.30	5.88	0.957
Auto-scaling	5	7.18	5.54	0.964

[a] Number of latent variables considered in the model. [b] Root mean square error of calibration. [c] Root mean square error of prediction. [d] R-square calculated on the calibration set.

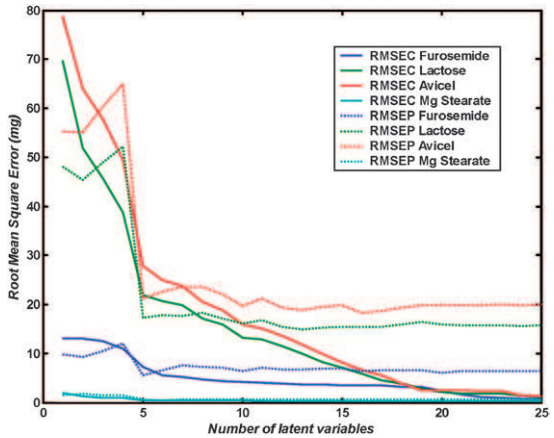

Fig. 4 Plot of the root mean square error of calibration and prediction, respectively, for the calibration and the validation set as a function of the number of latent variable considered in the partial least square model.

(RMSEP) for furosemide, and correlation coefficient (R^2) obtained for the different possibilities.

It is observed in Table 2 that the best combination based on our conditions is PLS coupled with auto-scaling. This combination presents the least number of latent variables with the lowest RMSEC and RMSEP (*i.e.* prediction errors) for furosemide. It should be noted that the same data pre-treatments also minimized the errors for the other constituents (data not shown).

The determination of an optimal number of latent variables is considered fundamentally essential for PCR or PLS, and can be evaluated by examining the plot of the RMSEC and RMSEP against the number of latent variables, shown in Fig. 4 for the PLS model with auto-scaling. It is then possible to observe that the calibration error (RMSEC) and the prediction error (RMSEP) drops significantly after four latent variables which is consistent with the number of compounds in our formulation (*i.e.* four). The RMSEP, which corresponds to prediction error of the validation set, passes through a minimum at five latent variables before it rises again, as is often observed when building PLS or PCR models. It is important to note that additional latent variables will start to include non-significant variation in the spectra, which will then increase the prediction error (*i.e.* RMSEP) since the regression model will start to model random noise and other non-correlated spectral data; this is typically referred to as over fitting in chemometrics terms.

In theory, the number of latent variables expected should be the same as the number of independent variables, which is four in this case (*i.e.* furosemide, Avicel®, lactose and magnesium stearate). However, in practice, it is often a few more than what the theory suggests, such that non-linear behavior of the signal and uncontrolled parameters in the calibration set can require additional latent variables to build a PCR or PLS model. Since manufacturing changes influence the LIBS signal, it should be possible to identify some "buried" variables using a more complex calibration set using a design of experiment (DOE) approach with an additional independent variable such as manufacturing changes (*e.g.* compression strength). The fact that the number of latent variables is five compared to four independent variables is a good indication of the validity of the developed PLS model with auto-scaling. Researchers from other spectroscopic fields have shown that near-infrared spectroscopy is influenced by the compression strength.[46] Hence, this could also be the case with molecular LIBS; consequently, this additional latent variable can be attributed to the compression strength. Present work on molecular LIBS shows that the compression strength is a significant independent variable that influences molecular LIBS signals.

Validation of the PLS model for five latent variables is presented in Fig. 5 for the comparison of the predicted mass in the formulation against the weighted mass for the prepared standard. The 1 : 1 correspondence line shows the precise agreement between the predicted values and the weighted mass. For the calibration set, the predicted values are in good agreement with the weighted mass for the calibration standards, the R^2 corresponding to all formulation ingredients for the calibration set is good with a noted value of 0.964. The worst cases are observed for the prediction of Avicel® and lactose (red and green points in Fig. 5), where bias between the predicted values and the weighted mass in formulation is less than 15% relative. Overall, these results are a breakthrough considering that the pharmaceutical manufacturers do not possess a process analytical sensor technology that enable the fast monitoring of excipients like Avicel® and lactose. For the other pharmaceutical ingredients, furosemide and magnesium stearate (blue and cyan points in Fig. 5), the relative accuracy for the prediction of the validation standards, expressed in percent is less than 4%. This is an excellent result showing that it is possible to predict accurately an API without the use or requirement of a traditional tag element in atomic LIBS. Collectively the statistics for RMSEC and RMSEP are shown in Table 3.

Nevertheless, the standard prediction for lactose and Avicel® reveals more scatter than for the API and lubricant compared to the weighted mass in the formulation. Considering the fact that the standards prepared in this study were made manually using mortar and pestle, weighting and non-automated compression methods, all these physical manipulations might incorporate additional random variations in the data sets. It may also indicate that several physical parameters may influence

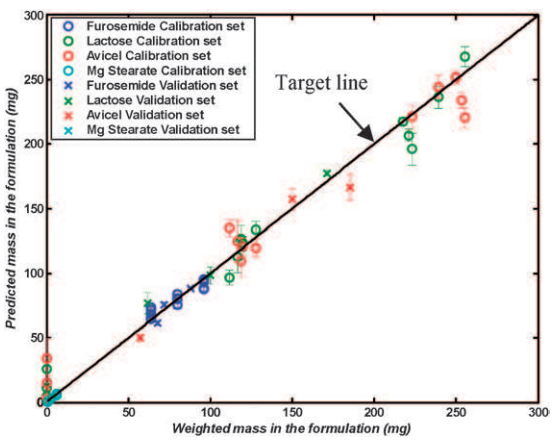

Fig. 5 Comparison between the predicted mass and the weighted mass for the different compounds entering in the studied furosemide formulation for the calibration set and the validation set for the PLS model using five latent variables. Points represent the mean of the six standard replicates and error bars represent the corresponding standard error.

Table 3 Statistics for PLS model using 5 latent variables for auto-scaled data

	RMSEC[a]/mg	RMSEP[b]/mg
Furosemide	7.2	5.5
Lactose	22	17
Avicel®	28	21
MgSt[c]	0.50	0.53

[a] Root mean square error of calibration. [b] Root mean square error of prediction. [c] Magnesium stearate.

the LIBS signal, as previously shown by other studies.[24,27] This places a greater importance on the use of standard calibration sets prepared under current good manufacturing practices (cGMP) conditions. The latter may have shown less spectral bias. Alternative studies in our laboratory using cGMP prepared formulation sample sets have provided preliminary data that seem to support this hypothesis. Future work will utilize cGMP sample sets for pharmaceutical studies which will require extensive validation and robustness testing to verify this hypothesis. Furthermore, the new calibration set should consider the potential manufacturing changes that may influence the molecular LIBS signals using a DOE approach that will spread the variance of these independent variables.

Preliminary pharmaceutical applications with atomic LIBS focused on the determination of the API or excipients in drug formulations with tag elements. Typically, it was difficult to accurately determine the API without matrix-matched standards due to the matrix effect. The analytical requirement for standard preparation offsets LIBS intrinsic analytical advantages of efficient direct determinations without sample preparation. Additionally, the direct determination of major excipients such as Avicel®, lactose, *etc.* was not readily accessible through traditional atomic spectroscopy techniques that were limited by sensitivity and selectivity issues. These spectroscopic and sensitivity limitations mostly confined LIBS to laboratory based confirmatory measurements, generally in a research setting. Applications such as the 3D-chemical mapping or accurate determination of coating thickness could provide important *in vitro* quality control tools to better assess *in vivo* drug bioavailability by predicting and or verifying drug dissolution. Our results indicate that it is now fully feasible to implement LIBS as an on-line or near-line PAT setting for in-process monitoring of manufacturing unit operations such as mixing or blending or even in process control. With the development of molecular LIBS and the potential for the simultaneous determination of API and excipients in complex matrices, the potential pharmaceutical applications should increase dramatically. Currently, no other PAT sensor technology or analytical technique can duplicate the broad applicability of this methodology. This suggests that molecular LIBS can actively monitor and provide efficient data for real time process monitoring over a wide range of manufacturing operations. Molecular LIBS could complement existing PAT sensor technologies such as near-infrared spectroscopy, chemical imaging and Raman spectroscopy. When coupled with standoff capability, molecular LIBS has the potential to dramatically enhance analytical capabilities in a PAT environment and evolve process understanding to a currently unimagined level, with efficient real time global (surface and interior) analysis of drug blends and final solid dosage forms.

Molecular LIBS may also provide a powerful pharmaceutical research tool that can enhance excipient screening, formulation development through novel dosage form assessment of excipient–API interactions, migration, tablet preparation, and ultimately formulation understanding that will provide a novel *in vitro* approach to *in vivo* performance.

Conclusions

We have demonstrated that LIBS coupled with chemometrics can provide the complete and simultaneous qualitative and quantitative prediction of all ingredients present in a pharmaceutical formulation. Molecular LIBS possess the capability to produce a combination of selective molecular, atomic and ionic emission signals that can differentiate between various molecules composing a complex matrix such as a pharmaceutical formulation.

Acknowledgements

We would like to acknowledge Martine Tourigny from Pharmalaser for the preparation of the calibration standards. Furthermore, we want to thank all Pharmalaser staff for their support and discussion on the application of LIBS to the analysis of pharmaceutical materials. We would like to thank Dr Mansoor A. Khan and Dr Ajaz S. Hussain for their support of LIBS research at the FDA.

References

1 F. R. Doucet, T. F. Belliveau, J. L. Fortier and J. Hubert, *Appl. Spectrosc.*, 2007, **61**, 327–332.
2 J. M. Anzano, I. B. Gornushkin, B. W. Smith and J. D. Winefordner, *Polym. Eng. Sci.*, 2000, **40**, 2423–2429.
3 R. Sattmann, I. Monch, H. Krause, R. Noll, S. Couris, A. Hatziapostolou, A. Mavromanolakis, C. Fotakis, E. Larrauri and R. Miguel, *Appl. Spectrosc.*, 1998, **52**, 456–461.
4 M. Oujja, A. Vila, E. Rebollar, J. F. Garcia and M. Castillejo, *Spectrochim. Acta, Part B*, 2005, **60**, 1140–1148.
5 F. Ferioli and S. G. Buckley, *Combust. Flame*, 2006, **144**, 435–447.
6 T. J. Lie, K. H. Kurniawan, D. P. Kurniawan, M. Pardede, M. M. Suliyanti, A. Khumaeni, S. A. Natiq, S. N. Abdulmadjid, Y. I. Lee, K. Kagawa, N. Idris and M. O. Tjia, *Spectrochim. Acta, Part B*, 2006, **61**, 104–112.
7 W. Schade, C. Bohling, K. Hohmann and D. Scheel, *Laser Part. Beams*, 2006, **24**, 241–247.
8 C. Bohling, D. Scheel, K. Hohmann, W. Schade, M. Reuter and G. Holl, *Appl. Opt.*, 2006, **45**, 3817–3825.
9 C. Respini Irwin, *Spectrosc.*, 2003, **18**, 50.
10 F. C. DeLucia, A. C. Samuels, R. S. Harmon, R. A. Walters, K. L. McNesby, A. LaPointe, R. J. Winkel and A. W. Miziolek, *IEEE Sens. J.*, 2005, **5**, 681–689.
11 F. C. DeLucia, R. S. Harmon, K. L. McNesby, R. J. Winkel and A. W. Miziolek, *Appl. Opt.*, 2003, **42**, 6148–6152.
12 C. Lopez Moreno, S. Palanco, J. J. Laserna, F. DeLucia, A. W. Miziolek, J. Rose, R. A. Walters and A. I. Whitehouse, *J. Anal. At. Spectrom.*, 2006, **21**, 55–60.
13 A. Portnov, S. Rosenwaks and I. Bar, *J. Lumin.*, 2003, **102**, 408–413.
14 A. Portnov, S. Rosenwaks and I. Bar, *Appl. Opt.*, 2003, **42**, 2835–2842.
15 P. Stavropoulos, A. Michalakou, G. Skevis and S. Couris, *Spectrochim. Acta, Part B*, 2005, **60**, 1092–1097.

16 M. Baudelet, L. Guyon, J. Yu, J. P. Wolf, T. Amodeo, E. Frejafon and P. Laloi, *Appl. Phys. Lett.*, 2006, **88**, 063901.
17 M. Baudelet, L. Guyon, J. Yu, J. P. Wolf, T. Amodeo, E. Frejafon and P. Laloi, *J. Appl. Phys.*, 2006, **99**, 163903.
18 C. A. Munson, F. C. De Lucia, T. Piehler, K. L. McNesby and A. W. Miziolek, *Spectrochim. Acta, Part B*, 2005, **60**, 1217–1224.
19 J. L. Gottfried, F. C. DeLucia, Jr, C. A. Munson and A. W. Miziolek, *J. Anal. At. Spectrom.*, 2008, **23**, 205–216.
20 F. C. DeLucia, Jr, J. L. Gottfried, C. A. Munson and A. W. Miziolek, *Spectrochim. Acta, Part B*, 2007, **62**, 1399–1404.
21 M. Baudelet, M. Boueri, J. Yu, S. S. Mao, V. Piscitelli, X. Mao and R. E. Russo, *Spectrochim. Acta, Part B*, 2007, **62**, 1329–1334.
22 V. I. Babushok, F. C. DeLucia, Jr, P. J. Dagdigian, J. L. Gottfried, C. A. Munson, M. J. Nusca and A. W. Miziolek, *Spectrochim. Acta, Part B*, 2007, **62**, 1321–1328.
23 M. Sabsabi and J. F. Bussière, *US Pat.*, 5 781 289, 1998.
24 J. F. Archambault, A. Vintiloiu and E. Kwong, *AAPS PharmSciTech*, 2005, **6**, E253–E261.
25 A. W. Miziolek, V. Palleschi and I. Schechter, *Laser-Induced Breakdown Spectroscopy (LIBS): Fundamentals and Applications*, Cambridge, New York, 2006.
26 M. D. Mowery, R. Sing, J. Kirsch, A. Razaghi, S. Bechard and R. A. Reed, *J. Pharm. Biomed. Anal.*, 2002, **28**, 935–943.
27 L. St Onge, J. F. Archambault, E. Kwong, M. Sabsabi and E. B. Vadas, *J. Pharm. Pharm. Sci.*, 2005, **8**, 272–288.
28 L. St Onge, E. Kwong, M. Sabsabi and E. B. Vadas, *J. Pharm. Biomed. Anal.*, 2004, **36**, 277–284.
29 L. St Onge, E. Kwong, M. Sabsabi and E. B. Vadas, *Spectrochim. Acta, Part B*, 2002, **57**, 1131–1140.
30 L. St Onge, R. Sing, S. Bechard and M. Sabsabi, *Appl. Phys. A*, 1999, **69**(Suppl. S), S913–S916.
31 D. Heuser and D. S. Walker, *J. Anal. At. Spectrom.*, 2004, **19**(7), 929–931.
32 R. L. Green, M. D. Mowery, J. A. Good, J. P. Higgins, S. M. Arrivo, K. McColough, A. Mateos and R. A. Reed, *Appl. Spectrosc.*, 2005, **59**, 340–347.
33 U. P. Agarwal and N. Kawai, *Appl. Spectrosc.*, 2005, **59**, 385–388.
34 P. Chalus, Y. Roggo, S. Walter and M. Ulmschneider, *Talanta*, 2005, **66**, 1294–1302.
35 H. Wikstrom, I. R. Lewis and L. S. Taylor, *Appl. Spectrosc.*, 2005, **59**, 934–941.
36 O. Berntsson, L. G. Danielsson and S. Folestad, *Anal. Chim. Acta*, 1998, **364**, 243–251.
37 F. C. Clarke, S. V. Hammond, R. D. Jee and A. C. Moffat, *Appl. Spectrosc.*, 2002, **56**, 1475–1483.
38 S. Romero Torres, J. D. Perez Ramos, K. R. Morris and E. R. Grant, *J. Pharm. Biomed. Anal.*, 2006, **41**, 811–819.
39 F. R. Doucet, M. Tourigny, M. Sabsabi, R. C. Lyon and P. J. Faustino, *AAPS J.*, 2006, **8**, R6019.
40 F. R. Doucet, L. St Onge, M. Tourigny, M. Sabsabi, R. C. Lyon and P. J. Faustino, *FDA Science Forum*, H-08, FDA Science Forum, Washington D.C., 2006.
41 P. Gemperline, *Pratical Guide to Chemometrics*, 2nd edn, Taylor & Francis Group, Boca Raton, 2006.
42 M. Holsapple, W. Farland, T. Landry, N. Monteiro-Riviere, J. Carter, N. Walker and K. Thomas, *Toxicol. Sci.*, 2005, **88**, 12–17.
43 P. Borm, D. Robbins, S. Haubold, T. Kuhlbusch, H. Fissan, K. Donaldson, R. Schins, V. Stone, W. Kreyling, J. Lademann, J. Krutmann, D. Warheit and E. Oberdorster, *Part. Fibre Toxicol.*, 2006, **3**, 1–35.
44 K. Thomas and P. Sayre, *Toxicol. Sci.*, 2005, **87**, 316–321.
45 S. Acquaviva, A. P. Caricato, M. L. DeGiorgi, G. Dinescu, A. Luches and A. Perrone, *J. Phys. B*, 1997, **30**, 4405–4414.
46 M. Hamad, J. T. Wang, A. Carlin, C. Ellison, E. Jefferson, R. C. Lyon, M. A. Khan and A. S. Hussain, *AAPS J.*, 2005, **7**, T3010.